Inorganic Chemistry
Article

Inorg. Chem. **2010**, *49*, 7323–7330 **7323**
DOI: 10.1021/ic1004775

Synthesis, Crystal Structure, and Characterization of a Heterometallic One-Dimensional Complex with Metal−Metal Bonds

Kazuhiro Uemura,*,† Kôichi Fukui,‡ Kana Yamasaki,‡ Kazuko Matsumoto,*,‡,§ and Masahiro Ebihara†

†*Department of Chemistry, Faculty of Engineering, Gifu University, Yanagido 1-1, Gifu 501-1193, Japan,* ‡*Department of Chemistry, School of Science and Engineering, Waseda University, 3-4-1 Ohkubo, Shinjuku, Tokyo 169-8555, Japan, and* §*Tokyo Chemical Industry Company, Ltd., 4-10-2 Nihonbashi-honcho, Chuo, Tokyo 103-0023, Japan*

Received March 12, 2010

The quasi-one-dimensional chain $[\{PtRh(TCM)_2(NH_3)_2Cl_{2.5}\}_2\{Pt_2(PVM)_2(NH_3)_4\}_2]_n(PF_6)_{6n}\cdot 2nH_2O$ (**Chain-2**; TCM = Cl_3CCONH^-, PVM = ^{t}BuCONH$^-$), which consists of Pt and Rh atoms, has been obtained from two dinuclear compounds, $[Pt_2(PVM)_2(NH_3)_4](PF_6)_2\cdot H_2O$ (**1**) and $[PtRh(TCM)_2(NH_3)_2Cl_3]$ (**2**). Single-crystal X-ray analysis showed that the dinuclear compounds stack with metal−metal bonds to form octameric units, Pt−Rh−Pt−Pt−Pt−Pt−Rh−Pt (Pt_6Rh_2), that are bridged by the Cl^- ion to be a quasi-one-dimensional chain. Elemental analysis, X-ray photoelectron spectroscopy, electron paramagnetic resonance (EPR), and magnetic susceptibility measurements showed that **Chain-2** has a mixed valency and one unpaired electron per octameric Pt_6Rh_2 unit. Taking into account the small observed g_{av} value ($g_{av} = 2.01$ at room temperature) obtained by EPR measurement and B3LYP density functional theory calculations of the model complex, oxidation states of the octameric unit are postulated to be $Pt^{3+}-Rh^{2.5+}-Pt^{2+}-Pt^{2+}-Pt^{2+}-Pt^{2+}-Rh^{2.5+}-Pt^{3+}$, where the EPR isotropic signal showed that the unpaired electron resides in the Rh d_{xy} orbitals (δ^* orbitals in Pt−Rh dinuclear parts) and hops from one Rh atom to another.

Introduction

One-dimensional (1D) metal complexes have been one of the intriguing subjects for the past several decades because of their unusual electrical properties,[1−3] including progressive resonance Raman spectra, large third-order nonlinear optical properties, and so on.[1d] Several infinite 1D metal complexes consisting of −M−M− bonds[2] and halogen-bridged −M−X− or −M−M−X− chains[3] have been synthesized and investigated so far, and finite 1D metal complexes, namely, extended metal atom chains (EMACs), have also been synthesized.[4] As found in $[Ni_4(\mu_4\text{-phdpda})_4]$ and $[Ni_7(\mu_7\text{-teptra})_4Cl_2]$ (H_2phdpda = *N*-phenyldipyridyldiamine and H_3teptra = tetrapyridyltriamine),[4b] the typical synthetic approach for

*To whom correspondence should be addressed. E-mail: k_uemura@gifu-u.ac.jp (K.U.), kmatsu@yf6.so-net.ne.jp (K.M.).

(1) (a) Miller, J. S. *Extended Linear Chain Compounds*; Plenum: New York, 1982; Vols. *1*−*3*. (b) Kitagawa, H.; Mitani, T. *Coord. Chem. Rev.* **1999**, *190*−*192*, 1169–1184. (c) Bera, J. K.; Dunbar, K. R. *Angew. Chem., Int. Ed.* **2002**, *41*, 4453–4457. (d) Yamashita, M.; Takaishi, S. *Bull. Chem. Soc. Jpn.* **2006**, *79*, 1820–1833.

(2) For recent reports on infinite 1D chains, see: (a) Finniss, G. M.; Canadell, E.; Campana, C.; Dunbar, K. R. *Angew. Chem., Int. Ed.* **1996**, *35*, 2772–2774. (b) Sakai, K.; Takeshita, M.; Tanaka, Y.; Ue, T.; Yanagisawa, M.; Kosaka, M.; Tsubomura, T.; Ato, M.; Nakano, T. *J. Am. Chem. Soc.* **1998**, *120*, 11353–11363. (c) Prater, M. E.; Pence, L. E.; Clerac, R.; Finniss, G. M.; Campana, C.; Auban-Senzier, P.; Jerome, D.; Canadell, E.; Dunbar, K. R. *J. Am. Chem. Soc.* **1999**, *121*, 8005–8016. (d) Cotton, F. A.; Dikarev, E. V.; Petrukhina, M. A. *J. Organomet. Chem.* **2000**, *596*, 130–135. (e) Cotton, F. A.; Dikarev, E. V.; Petrukhina, M. A. *J. Chem. Soc., Dalton Trans.* **2000**, 4241–4243. (f) Pruchnik, F. P.; Jakimowicz, P.; Ciunik, Z.; Stanislawek, K.; Oro, L. A.; Tejel, C.; Ciriano, M. A. *Inorg. Chem. Commun.* **2001**, *4*, 19–22. (g) Pruchnik, F. P.; Jakimowicz, P.; Ciunik, Z. *Inorg. Chem. Commun.* **2001**, *4*, 726–729. (h) Sakai, K.; Ishigami, E.; Konno, Y.; Kajiwara, T.; Ito, T. *J. Am. Chem. Soc.* **2002**, *124*, 12088–12089. (i) Mitsumi, M.; Umebayashi, S.; Ozawa, Y.; Tadokoro, M.; Kawamura, H.; Toriumi, K. *Chem. Lett.* **2004**, *33*, 970–971. (j) Mitsumi, M.; Goto, H.; Umebayashi, S.; Ozawa, Y.; Kobayashi, M.; Yokoyama, T.; Tanaka, H.; Kuroda, S.-i.; Toriumi, K. *Angew. Chem., Int. Ed.* **2005**, *44*, 4164–4168.

(3) For recent reports on halogen-bridged infinite 1D chains, see: (a) Yamashita, M.; Miya, S.; Kawashima, T.; Manabe, T.; Sonoyama, T.; Kitagawa, H.; Mitani, T.; Okamoto, H.; Ikeda, R. *J. Am. Chem. Soc.* **1999**, *121*, 2321–2322. (b) Kitagawa, H.; Onodera, N.; Sonoyama, T.; Yamamoto, M.; Fukawa, T.; Mitani, T.; Seto, M.; Maeda, Y. *J. Am. Chem. Soc.* **1999**, *121*, 10068–10080. (c) Mitsumi, M.; Murase, T.; Kishida, H.; Yoshinari, T.; Ozawa, Y.; Toriumi, K.; Sonoyama, T.; Kitagawa, H.; Mitani, T. *J. Am. Chem. Soc.* **2001**, *123*, 11179–11192. (d) Mitsumi, M.; Kitamura, K.; Morinaga, A.; Ozawa, Y.; Kobayashi, M.; Toriumi, K.; Iso, Y.; Kitagawa, H.; Mitani, T. *Angew. Chem., Int. Ed.* **2002**, *41*, 2767–2771. (e) Matsuzaki, H.; Matsuoka, T.; Kishida, H.; Takizawa, K.; Miyasaka, H.; Sugiura, K.; Yamashita, M.; Okamoto, H. *Phys. Rev. Lett.* **2003**, *90*, 0464011–0464014. (f) Yamashita, M.; Kawakami, D.; Matsunaga, S.; Nakayama, Y.; Sasaki, M.; Takaishi, S.; Iwahori, F.; Miyasaka, H.; Sugiura, K.; Wada, Y.; Miyamae, H.; Matsuzaki, H.; Okamoto, H.; Tanaka, H.; Marumoto, K.; Kuroda, S. *Angew. Chem., Int. Ed.* **2004**, *43*, 4763–4767. (g) Kawakami, D.; Yamashita, M.; Matsunaga, S.; Takaishi, S.; Kajiwara, T.; Miyasaka, H.; Sugiura, K.-i.; Matsuzaki, H.; Okamoto, H.; Wakabayashi, Y.; Sawa, H. *Angew. Chem., Int. Ed.* **2006**, *45*, 7214–7217. (h) Takaishi, S.; Kawakami, D.; Yamashita, M.; Sasaki, M.; Kajiwara, T.; Miyasaka, H.; Sugiura, K.-i.; Wakabayashi, Y.; Sawa, H.; Matsuzaki, H.; Kishida, H.; Okamoto, H.; Watanabe, H.; Tanaka, H.; Marumoto, K.; Ito, H.; Kuroda, S.-i. *J. Am. Chem. Soc.* **2006**, *128*, 6420–6425. (i) Kobayashi, A.; Kojima, T.; Ikeda, R.; Kitagawa, H. *Inorg. Chem.* **2006**, *45*, 322–327.

Published on Web 07/20/2010

EMACs depends on designed organic ligands, where some metals are aligned to be finite 1D chains by the coordination conditions. In contrast, in the case of infinite chains, the approach depends on the metal oxidation states: half-filled (d^7) and filled (d^8) d_{z^2} orbitals are superimposed to form σ bonds and infinitely crystallized as in $K_2[Pt(CN)_4]Br_{0.3}\cdot 3.2H_2O$.[1a] Therefore, most infinite 1D metal complexes have made use of $Rh^{+/2+}$ and/or $Pt^{2+/3+}$, where partial oxidation or reduction of the d_{z^2} orbitals attributed to the $d^7 \leftrightarrow d^8$ redox changes are utilized toward the formation of partially filled valence bands along the z axis.[1]

Amidate-bridged tetranuclear platinum complexes (Pt_4) have been widely studied since the 1970s, revealing characteristic crystal structures and unique properties.[5−8] A noteworthy feature is that their average oxidation states in Pt atoms are reversibly oxidized and reduced to be Pt^{2+},[6] $Pt^{2.25+}$,[7] and $Pt^{2.5+}$.[8] In particular, compounds containing $Pt^{2.25+}$, so-called "platinum blue", have one unpaired electron that is delocalized over four Pt atoms.[7] Because the unpaired electron resides in a σ^* orbital, superimposed σ^* orbitals are expected to afford partially filled valence bands. Consequently, some efforts to obtain extended "platinum blue" have been made, and octanuclear platinum complexes[9] and an infinite carboxylate-bridged platinum chain[2h] have been reported to date.

Previously, we have unprecedentedly obtained and reported a crystal structure of the infinite 1D heterometallic complex $[\{PtRh(PVM)_2(NH_3)_2Cl_{2.5}\}_2\{Pt_2(PVM)_2(NH_3)_4\}_2]_n(PF_6)_{6n}\cdot 2n MeOH\cdot 2nH_2O$ (**Chain-1**; PVM = ^{t}BuCONH$^-$), which consists of octameric units Pt−Rh−Pt−Pt−Pt−Pt−Rh−Pt (Pt_6Rh_2).[10] The octameric unit is composed of two types of dinuclear PVM-bridged complexes, [Pt−Rh] and [Pt−Pt], where each unit is bridged by Cl^- ions, expressed as −[Pt−Rh]−[Pt−Pt]−[Pt−Pt]−[Rh−Pt]−Cl−. Thus, **Chain-1** is regarded as an extended Pt_4, where the inner tetranuclear platinum complexes are connected by [Pt−Rh] complexes. **Chain-1** was synthesized by simply mixing *cis*-$[Pt(PVM)_2(NH_3)_2]\cdot 2H_2O$, $RhCl_3\cdot 3H_2O$, and $NaPF_6$ in MeOH and crystallized through the formation of [Pt−Rh] and [Pt−Pt] complexes.[10a] **Chain-1** is a unique paramagnetic chain composed of two types of metal. A preliminary study of the electron paramagnetic resonance (EPR) spectra of **Chain-1** showed that one unpaired spin per octanuclear unit occupies the Rh d_{xy} orbitals and hops from one Rh atom to another in the Pt_6Rh_2 unit;[10] however, no further detailed EPR measurement was possible because of the lack of crystal stability. Here, we report the synthesis, crystal structure, and intervalence spin-hopping dynamics observation of a novel mixed-valent 1D chain, $[\{PtRh(TCM)_2(NH_3)_2Cl_{2.5}\}_2\{Pt_2(PVM)_2(NH_3)_4\}_2]_n(PF_6)_{6n}\cdot 2nH_2O$ (**Chain-2**; TCM = Cl_3CCONH^-). The success in obtaining **Chain-2** implies that this type of heterometallic 1D chain could be rationally synthesized. **Chain-2** was further characterized by X-ray photoelectron spectroscopy (XPS), magnetic susceptibility, temperature-dependent EPR measurements, and density functional theory (DFT) calculations.

Experimental Section

Materials. Pivalonitrile, trichloroacetonitrile, and sodium hexafluorophosphate were obtained from Tokyo Kasei Industrial Co. Rhodium(III) chloride trihydrate was obtained from Kanto Chemical Co. Potassium tetrachloroplatinate(II) was obtained from Tanaka Kikinzoku Co. Silver hexafluorophosphate was obtained from Aldrich Co. *cis*-$[PtCl_2(NH_3)_2]$ was synthesized according to a previous procedure.[11]

Synthesis of $[Pt_2(PVM)_2(NH_3)_4](PF_6)_2\cdot H_2O$ (1). *cis*-$[Pt(PVM)_2(NH_3)_2]\cdot 2H_2O$ was obtained according to a previous procedure.[12] Instead of the previous procedure,[10a] compound **1** was obtained with higher yield according the following procedure. An aqueous solution (4 mL) of *cis*-$[PtCl_2(NH_3)_2]$ (1.0 mmol, 0.30 g) was stirred with 2 equiv of $AgPF_6$ (2.0 mmol, 0.51 g) for 12 h in the dark, and AgCl was then removed by filtration. The colorless filtrate was stirred with 2 equiv of *cis*-$[Pt(PVM)_2(NH_3)_2]\cdot 2H_2O$ (1.0 mmol, 0.47 g) for 2 min at 40 °C. The resulting suspension was filtered to obtain a light-blue product. Yield: 70%.

Synthesis of $[\{PtRh(TCM)_2(NH_3)_2Cl_{2.5}\}_2\{Pt_2(PVM)_2(NH_3)_4\}_2]_n(PF_6)_{6n}\cdot 2nH_2O$ (Chain-2). $[PtRh(TCM)_2(NH_3)_2Cl_3]$ (**2**) was obtained according to a previous procedure.[13] A MeOH solution (0.5 mL) of **1** (5 μmol, 4.8 mg) and $NaPF_6$ (25 μmol, 4.2 mg) was added to a solution of **2** (5 μmol, 3.8 mg) in MeOH (0.5 mL). The mixed solution was allowed to stand in a tube for 1 month. Dark-brown crystals were separated, washed with water, and dried. Yield: 20%. Elem anal. Calcd for $C_{28}H_{84}Cl_{17}F_{36}N_{20}O_{10}P_6Pt_6Rh_2$: C, 9.07; H, 2.28; N, 7.55. Found: C, 9.15; H, 2.19; N, 7.63.

Physical Measurements. The XPS measurements were carried out on a JEOL JPS-9010 spectrometer at room temperature. Binding energies were measured relative to the C 1s peak

(4) For recent reports on finite 1D metal complexes, see: (a) Tejel, C.; Ciriano, M. A.; López, J. A.; Lahoz, F. J.; Oro, L. A. *Angew. Chem., Int. Ed.* **1998**, *37*, 1542–1545. (b) Lai, S.-Y.; Lin, T.-W.; Chen, Y.-H.; Wang, C.-C.; Lee, G.-H.; Yang, M.-h.; Leung, M.-k.; Peng, S.-M. *J. Am. Chem. Soc.* **1999**, *121*, 250–251. (c) Clerac, R.; Cotton, F. A.; Dunbar, K. R.; Lu, T.; Murillo, C. A.; Wang, X. *J. Am. Chem. Soc.* **2000**, *122*, 2272–2278. (d) Tejel, C.; Ciriano, M. A.; Villarroya, B. E.; Gelpi, R.; López, J. A.; Lahoz, F. J.; Oro, L. A. *Angew. Chem., Int. Ed.* **2001**, *40*, 4084–4086. (e) Murahashi, T.; Uemura, T.; Kurosawa, H. *J. Am. Chem. Soc.* **2003**, *125*, 8436–8437. (f) Goto, E.; Begum, R. A.; Zhan, S.; Tanase, T.; Tanigaki, K.; Sakai, K. *Angew. Chem., Int. Ed.* **2004**, *43*, 5029–5032. (g) Ruffer, T.; Ohashi, M.; Shima, A.; Mizomoto, H.; Kaneda, Y.; Mashima, K. *J. Am. Chem. Soc.* **2004**, *126*, 12244–12245. (h) Tejel, C.; Ciriano, M. A.; Villarroya, B. E.; Lopez, J. A.; Lahoz, F. J.; Oro, L. A. *Angew. Chem., Int. Ed.* **2003**, *42*, 529–532.

(5) (a) Tejel, C.; Ciriano, M. A.; Oro, L. A. *Chem.—Eur. J.* **1999**, *5*, 1131–1135. (b) Matsumoto, K.; Sakai, K. *Adv. Inorg. Chem.* **2000**, *49*, 375–427.

(6) For tetranuclear platinum(2+) chains, see: (a) Hollis, L. S.; Lippard, S. J. *J. Am. Chem. Soc.* **1981**, *103*, 1230–1232. (b) Laurent, J.-P.; Lepage, P.; Dahan, F. *J. Am. Chem. Soc.* **1982**, *104*, 7335–7336. (c) Hollis, L. S.; Lippard, S. J. *Inorg. Chem.* **1983**, *22*, 2600–2604. (d) Hollis, L. S.; Lippard, S. J. *J. Am. Chem. Soc.* **1983**, *105*, 3494–3503. (e) Matsumoto, K.; Miyamae, H.; Moriyama, H. *Inorg. Chem.* **1989**, *28*, 2959–2964.

(7) For tetranuclear platinum(2.25+) chains (platinum blue), see: (a) Barton, J. K.; Rabinowitz, H. N.; Szalda, D. J.; Lippard, S. J. *J. Am. Chem. Soc.* **1977**, *99*, 2827–2829. (b) Barton, J. K.; Szalda, D. J.; Rabinowitz, H. N.; Waszczak, J. V.; Lippard, S. J. *J. Am. Chem. Soc.* **1979**, *101*, 1434–1441. (c) O'Halloran, T. V.; Roberts, M. M.; Lippard, S. J. *J. Am. Chem. Soc.* **1984**, *106*, 6427–6428. (d) Mascharak, P. K.; Williams, I. D.; Lippard, S. J. *J. Am. Chem. Soc.* **1984**, *106*, 6428–6430. (e) Matsumoto, K.; Matsunami, J.; Urata, H. *Chem. Lett.* **1993**, 597–600. (f) Sakai, K.; Tanaka, Y.; Tsuchiya, Y.; Hirata, K.; Tsubomura, T.; Iijima, S.; Bhattacharjee, A. *J. Am. Chem. Soc.* **1998**, *120*, 8366–8379.

(8) For tetranuclear platinum(2.5+) chains, see: (a) Matsumoto, K.; Fuwa, K. *J. Am. Chem. Soc.* **1982**, *104*, 897–898. (b) Matsumoto, K.; Takahashi, H.; Fuwa, K. *Inorg. Chem.* **1983**, *22*, 4086–4090.

(9) (a) Sakai, K.; Matsumoto, K. *J. Am. Chem. Soc.* **1989**, *111*, 3074–3075. (b) Matsumoto, K.; Sakai, K.; Nishio, K.; Tokisue, Y.; Ito, R.; Nishide, T.; Shichi, Y. *J. Am. Chem. Soc.* **1992**, *114*, 8110–8118.

(10) (a) Uemura, K.; Fukui, K.; Nishikawa, H.; Arai, S.; Matsumoto, K.; Oshio, H. *Angew. Chem., Int. Ed.* **2005**, *44*, 5459–5464. (b) Uemura, K.; Fukui, K.; Yamasaki, K.; Matsumoto, K. *Sci. Technol. Adv. Mater.* **2006**, *7*, 461–467.

(11) Dkhara, S. C. *Indian J. Chem.* **1970**, *8*, 193–194.

(12) Chen, W.; Matsumoto, K. *Inorg. Chim. Acta* **2003**, *342*, 88–96.

(13) (a) Uemura, K.; Yamasaki, K.; Fukui, K.; Matsumoto, K. *Inorg. Chim. Acta* **2007**, *360*, 2623–2630. (b) Uemura, K.; Yamasaki, K.; Fukui, K.; Matsumoto, K. *Eur. J. Inorg. Chem.* **2007**, 809–815.

(284.8 eV) of an internal hydrocarbon. The X-band EPR spectra were recorded on a JEOL JES-PX1060 spectrometer. Magnetic susceptibility measurement was carried out in the temperature range 2−275 K with a magnetometer (Quantum Design MPMS-7) equipped with a SQUID sensor. The UV−vis reflection spectra were recorded on a Shimadzu UV-3101PC spectrophotometer over the range from 400 to 800 nm at room temperature.

X-ray Structure Determination for Chain-2. Measurement were carried out on a Bruker SMART APEX CCD diffractometer equipped with a normal focus Mo-target X-ray tube (λ = 0.710 73 Å) operated at 2000 W power (50 kV, 40 mA) and a CCD two-dimensional detector. A total of 1315 frames were collected with a scan width of 0.3° in ω with an exposure time of 30 s/frame. The frames were integrated with the *SAINT* software package with a narrow-frame algorithm.[14] Absorption correction was applied by using *SADABS*.[15] The structure was solved by direct methods[16] with subsequent difference Fourier syntheses and refinement with the *SHELXTL* software package.[17] The O atoms (O9 and O10) of the water molecules and N4, N10, N12, N17, N18, C5, C16, and C22 were refined isotropically. The atoms O3, O7, N9, N19, C11, C12, C25, C26, Cl4−6, and Cl12−14 in trichloroacetoamidate were isotropically refined under rigid conditions because of high disorders. Because guest molecules were severely disordered, all PF_6^- anions could not be located in the difference Fourier maps. The other non-H atoms were refined anisotropically, and all H atoms were placed in ideal positions. The crystal data and structure refinement results are summarized in Table 1.

DFT Calculation. The electronic structure of model compound $[\{PtRh(PVM)_2(NH_3)_2Cl_2\}_2\{Pt_2(PVM)_2(NH_3)_4\}_2]^{6+}$ was calculated with the DFT method using the B3LYP functional[18] with the *Gaussian03* program package.[19] For Pt and Rh, the LANL2DZ basis set was used together with the effective core potential of Hay and Wadt.[20] For the other elements, the 6-31G* basis sets[21] were selected. The model of $[\{PtRh(PVM)_2(NH_3)_2Cl_2\}_2\{Pt_2(PVM)_2(NH_3)_4\}_2]^{6+}$ was generated by using the geometry parameters obtained from crystal structure data of **Chain-1**.[10a]

Results and Discussion

Synthetic Procedure. Chain-1 consists of two types of dinuclear complexes, $[Pt_2(PVM)_2(NH_3)_4]^{2+}$ ([Pt−Pt]) and $[PtRh(PVM)_2(NH_3)_2Cl_2]$ ([Pt−Rh]), where each complex is stacked and aligned in the order −[Pt−Rh]−[Pt−Pt]−[Pt−Pt]−[Rh−Pt]−Cl−.[10] As a candidate for a new 1D chain, we have selected the less electron-donating TCM ligand as bridging ligands for [Pt−Rh] complexes in place of the PVM ligand, for the purpose of lowering the highest occupied molecular orbital (HOMO) level around the Rh atoms. To substitute organic ligands in **Chain-1**, a rational synthetic method for **Chain-1** is necessary, and we succeeded in obtaining the expected compounds by simply mixing dinuclear complexes, [Pt−Pt] and [Pt−Rh], in a ratio of 1:1 (Scheme 1). Brown single crystals of **Chain-2** with a metallic luster were also obtained by mixing two dinuclear complexes, **1** and **2**, followed by evaporation of the solution in air. The oxidation states of the metal ions in **1** and **2** are Pt^{2+}−Pt^{2+} and Pt^{2+}−Rh^{3+}, respectively, as reported previously.[13b]

Table 1. Crystallographic Data and Structure Refinements for **Chain-2**

empirical formula	$C_{28}H_{80}Cl_{17}F_{12}N_{20}O_{10}P_2Pt_6Rh_2$
fw	3126.07
cryst syst	triclinic
space group	$P\bar{1}$
a (Å)	13.455(6)
b (Å)	17.782(8)
c (Å)	21.349(10)
α (deg)	74.622(9)
β (deg)	79.551(9)
γ (deg)	79.929(9)
V (Å^3)	4800(4)
Z	2
D_c (Mg m^{-3})	2.163
abs coeff (mm^{-1})	9.618
F(000)	2906
cryst size (mm^3)	0.45 × 0.30 × 0.10
measd reflns	29 690
indep reflns	20 556 [R_{int} = 0.0757]
GOF on F^2	1.043
R [$I > 2\sigma(I)$][a]	R1 = 0.1145, wR2 = 0.2938

[a] $R1 = \sum(|F_o|-|F_c|)/\sum(|F_o|)$, $wR2 = \{\sum[w(F_o^2-F_c^2)^2]/\sum[w(F_o^2)^2]\}^{1/2}$.

Scheme 1

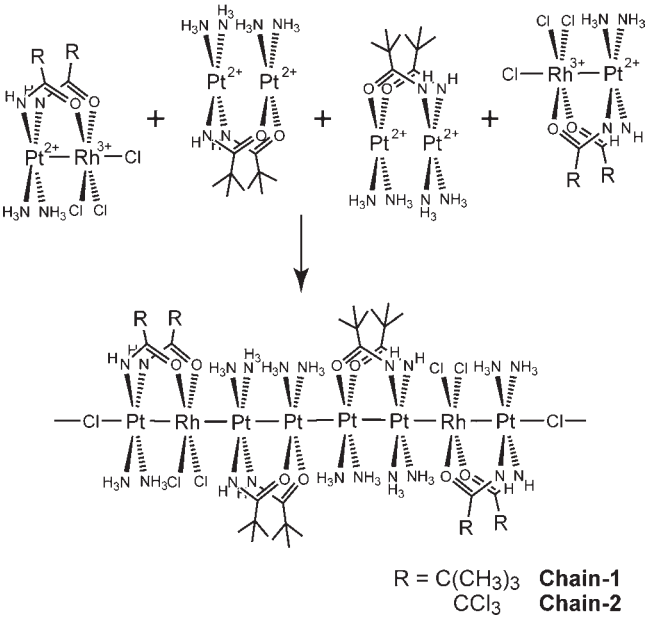

Crystal Structure. **Chain-2** crystallizes in the triclinic space group $P\bar{1}$ with two $[PtRh(TCM)_2(NH_3)_2Cl_2]$-$[Pt_2(PVM)_2(NH_3)_4]_2[PtRh(TCM)_2(NH_3)_2Cl_2]$ fragments

(14) *SMART & SAINT Software Pakage*, version 5.625; Siemens Energy & Automation, Inc., Analytical Instrumentation: Madison, WI, 2001.
(15) Sheldrick, G. M. *SADABS, Software for Empirical Absorption Corrections*; University of Göttingen: Göttingen, Germany, 1996.
(16) Altomare, A.; Cascarano, G.; Giacovazzo, C.; Guagliardi, A.; Burla, M. C.; Polidori, G.; Camalli, M. *J. Appl. Crystallogr.* **1994**, *27*, 435–436.
(17) Sheldrick, G. M. *Acta Crystallogr.* **2008**, *A64*, 112–122.
(18) (a) Becke, A. D. *J. Chem. Phys.* **1993**, *98*, 5648–5652. (b) Miehlich, B.; Savin, A.; Stoll, H.; Preuss, H. *Chem. Phys. Lett.* **1989**, *157*, 200–206. (c) Lee, C. T.; Yang, W. T.; Parr, R. G. *Phys. Rev. B* **1988**, *37*, 785–789.
(19) Frisch, M. J.; Trucks, G. W.; Schlegel, H. B.; Scuseria, G. E.; Robb, M. A.; Cheeseman, J. R.; Montgomery, J. A., Jr.; Vreven, T.; Kudin, K. N.; Burant, J. C.; Millam, J. M.; Iyengar, S. S.; Tomasi, J.; Barone, V.; Mennucci, B.; Cossi, M.; Scalmani, G.; Rega, N.; Petersson, G. A.; Nakatsuji, H.; Hada, M.; Ehara, M.; Toyota, K.; Fukuda, R.; Hasegawa, J.; Ishida, M.; Nakajima, T.; Honda, Y.; Kitao, O.; Nakai, H.; Klene, M.; Li, X.; Knox, J. E.; Hratchian, H. P.; Cross, J. B.; Bakken, V.; Adamo, C.; Jaramillo, J.; Gomperts, R.; Stratmann, R. E.; Yazyev, O.; Austin, A. J.; Cammi, R.; Pomelli, C.; Ochterski, J. W.; Ayala, P. Y.; Morokuma, K.; Voth, G. A.; Salvador, P.; Dannenberg, J. J.; Zakrzewski, V. G.; Dapprich, S.; Daniels, A. D.; Strain, M. C.; Farkas, O.; Malick, D. K.; Rabuck, A. D.; Raghavachari, K.; Foresman, J. B.; Ortiz, J. V.; Cui, Q.; Baboul, A. G.; Clifford, S.; Cioslowski, J.; Stefanov, B. B.; Liu, G.; Liashenko, A.; Piskorz, P.; Komaromi, I.; Martin, R. L.; Fox, D. J.; Keith, T.; Al-Laham, M. A.; Peng, C. Y.; Nanayakkara, A.; Challacombe, M.; Gill, P. M. W.; Johnson, B.; Chen, W.; Wong, M. W.; Gonzalez, C.; Pople, J. A. *Gaussian 03*, revision B.05; Gaussian, Inc.: Wallingford, CT, 2004.
(20) Hay, P. J.; Wadt, W. R. *J. Chem. Phys.* **1985**, *82*, 299–310.
(21) Hariharan, P. C.; Pople, J. A. *Theor. Chim. Acta* **1973**, *28*, 213–222.

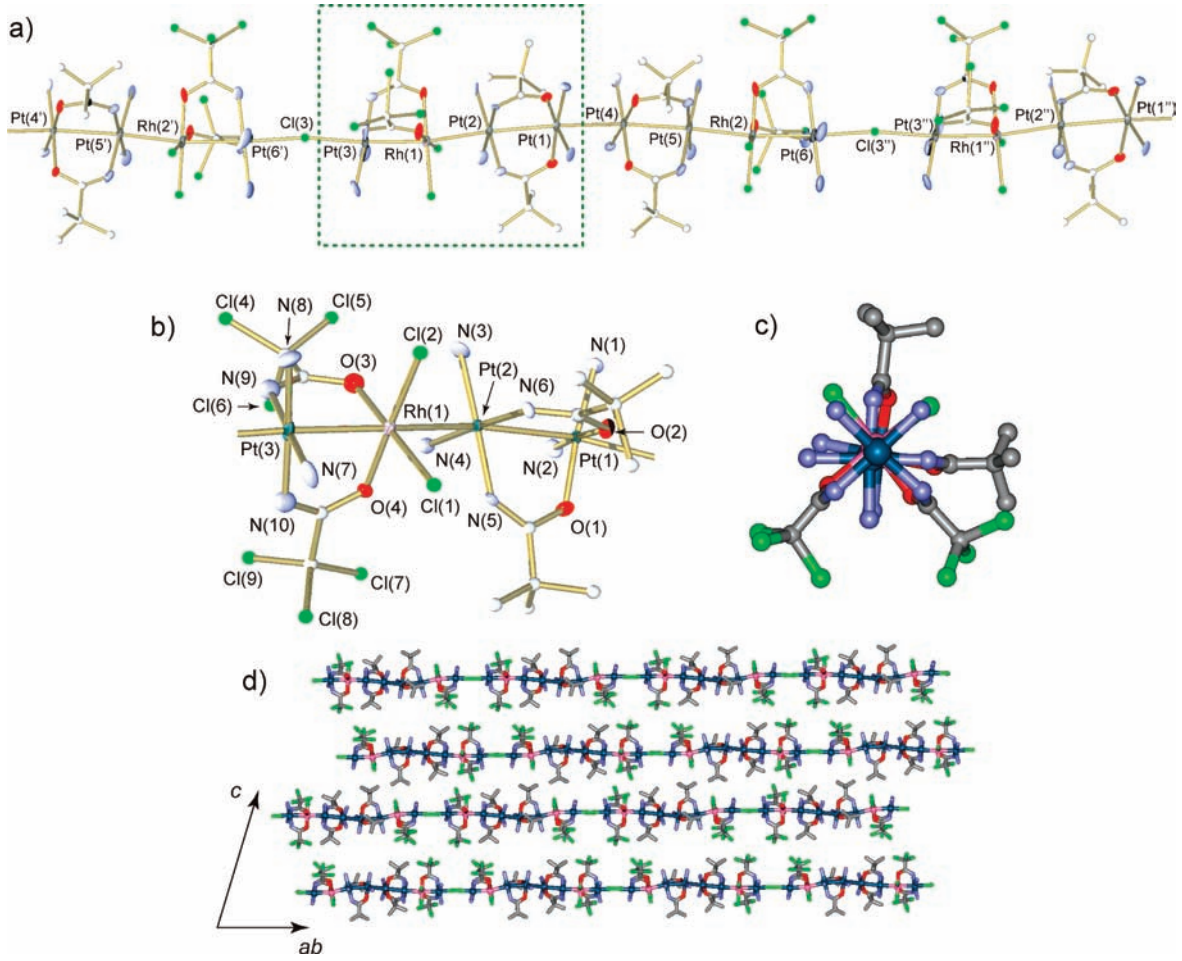

Figure 1. (a) Crystal structure of **Chain-2**. (b) Amplified view of the green dotted square in part a showing the metal−metal bond between two dinuclear compounds, $[PtRh(TCM)_2(NH_3)_2Cl_2]$ and $[Pt_2(PVM)_2(NH_3)_4]$. (c) View along the metal−metal bond between $[PtRh(TCM)_2(NH_3)_2Cl_2]$ and $[Pt_2(PVM)_2(NH_3)_4]$. (d) Crystal packing of the 1D chains in **Chain-2**. All chains are parallel in the crystal. The H atoms, PF_6^- ions, and water molecules are omitted for clarity.

per unit cell, comprising infinite linear chains based on the Pt_6Rh_2 unit, [Pt(3)−Rh(1)]−[Pt(2)−Pt(1)]−[Pt(4)−Pt(5)]−[Rh(2)−Pt(6)]−Cl (Figure 1a).[22] The inner $[Pt_2(PVM)_2(NH_3)_4]$ and outer $[PtRh(TCM)_2(NH_3)_2Cl_2]$ dinuclear complexes of **Chain-2** are doubly bridged with PVM and TCM ligands, respectively (Figure 1b). The central interdimer interaction is reinforced by four hydrogen bonds between the O atoms of PVM and the H atoms of the ammine ligands. The distances between the PVM-bridged Pt atoms [Pt(1)−Pt(2) and Pt(4)−Pt(5)] are 2.8445(15) and 2.8062(15) Å, respectively, and are shorter than the inner nonbridged Pt(1)−Pt(4) distance of 2.9793(16) Å. The outer dimers, $[PtRh(TCM)_2(NH_3)_2Cl_2]$ [Pt(3)−Rh(1) = 2.605(2) Å; Pt(6)−Rh(2) = 2.602(2) Å], are bonded to both ends of the central tetranuclear platinum unit with distances of Pt(2)−Rh(1) = 2.742(2) Å and Pt(5)−Rh(2) = 2.715(2) Å and a twist angle of about 45° (Figure 1c). The Pt_6Rh_2 units are further bridged by Cl^- ligands [Pt(3)−Cl(3) = 2.563(8) Å; Pt(6)−Cl(3″) = 2.588(8) Å] to give a pseudo-1D infinite chain, −[Pt−Rh]−[Pt−Pt]−[Pt−Pt]−[Rh−Pt]−Cl−. The other metal arrangements are unlikely because higher R values were obtained when different models were used. As shown in Figure 1d, each 1D chain in the crystal runs parallel to the [001] direction. Despite the high degree of PF_6^- disorder in the crystal lattice, elemental analysis shows six PF_6^- ions per octameric unit, and the unit formula is **Chain-2**, which corresponds to a total metal charge of 19+ for the Pt_6Rh_2 unit.

Chain-2 is structurally analogous to **Chain-1**, comprising infinite linear chains based on the Pt_6Rh_2 unit, −[Pt−Rh]−[Pt−Pt]−[Pt−Pt]−[Rh−Pt]−Cl−. Table 2 summarizes the metal−metal distances (d_{1-7}), tilt between the coordination planes (θ_{1-7}), and torsion angles (φ_{1-7}) according to the definition in Scheme 2. The dominant differences between **Chain-1** and **Chain-2** are d_4 and φ_4, which correspond to the unbridged Pt−Pt distance and torsion angle among the inner [Pt−Pt] compounds, respectively. The distance d_4 in **Chain-2** [2.9793(16) Å] is shorter than that in **Chain-1** [3.0634(10) Å]. The decrease in the Pt−Pt distance with an increase in the average oxidation state of platinum is widely observed in this class of compounds.[8a] Both the inter- (d_4) and intradimer (d_3 and d_5)

(22) **Chain-2** is easily decomposed to **1** and **2** when dissolved in MeOH, which was confirmed with electrospray ionization mass spectrometry (ESI-MS). As shown in Figure S1 in the Supporting Information, the peaks attributed to the two kinds of dinuclear complexes, $\{[PtRh(TCM)_2(NH_3)_2Cl_2]\cdot MeOH\}^+$ (m/z = 757) and $\{[Pt_2(PVM)_2(NH_3)_4](PF_6)\}^+$ (m/z = 803), are clearly observed. Hence, the results of both single-crystal X-ray analysis and ESI-MS reveal that **Chain-2** comprises **1** and **2**, indicating that the synthetic strategy succeeded in substituting amidate ligands from PVM (**Chain-1**) to TCM (**Chain-2**).

Table 2. Comparison of Selected Bond Distances (Å) and Angles (deg) in **Chain-1** and **Chain-2**

	d_1	d_2	d_3	d_4	d_5	d_6	d_7
Chain-1	2.5987(11)	2.7337(11)	2.8450(7)	3.0634(10)	2.8450(7)	2.7337(11)	2.5987(11)
Chain-2	2.605(2)	2.742(2)	2.8445(15)	2.9793(16)	2.8062(15)	2.715(2)	2.602(2)
	θ_1	θ_2	θ_3	θ_4	θ_5	θ_6	θ_7
Chain-1	17.7	5.7	28.1	0.0	28.1	5.7	17.7
Chain-2	17.2	5.3	29.6	1.8	24.5	4.2	16.2
	φ_1	φ_2	φ_3	φ_4	φ_5	φ_6	φ_7
Chain-1	7	136	2	180	2	136	7
Chain-2	7	143	10	153	3	137	17

Scheme 2

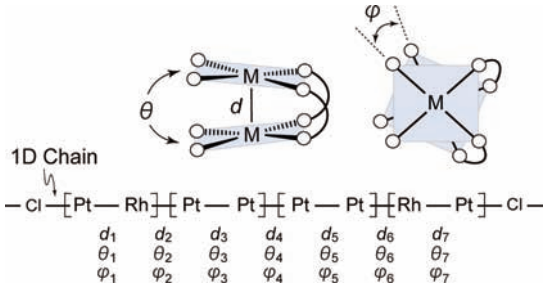

Pt−Pt distances in **Chain-2** are longer than the corresponding lengths in platinum blue $[Pt_4(PVM)_4(NH_3)_8](PF_6)_4(ClO_4)\cdot 2H_2O$ [inter, 2.8603(12) Å; intra, 2.8039(9) Å] with average $Pt^{2.25+}$ but still much shorter than those in $[Pt_2(PVM)_2(NH_3)_4](PF_6)_2\cdot 2H_2O$ [inter, 3.1256(12) Å; intra, 2.9546(11) Å] with average Pt^{2+}.[10]

Electronic Structure. The electronic structure of **Chain-1** shows that the singly occupied molecular orbital (SOMO) in **Chain-1** is attributed most likely to the Rh^{2+} d_{xy} orbital raised in energy above d_{z^2} through π interactions with the amidate ligands, which is revealed by the EPR result at room temperature.[10] That electronic structure was deduced from the smaller g_{av} value of **Chain-1** than those of the d_{z^2}-type platinum(3+) complexes[23] and rhodium(2+) complex,[24] which are interpreted in terms of a d_{z^2} hole state with an admixture of the lower-lying d_{xz} and d_{yz} states because of spin−orbit coupling.[25] No further detailed measurement for **Chain-1** was possible because of the lack of crystal stability, resulting from the MeOH molecules in the crystal of **Chain-1**. On the other hand, the crystal of **Chain-2** is relatively stable, accommodating water molecules but no MeOH, and a modified electronic structure is anticipated considering the difference of bridging ligands between **Chain-1** and **Chain-2**.

To determine the metal oxidation states in the Pt_6Rh_2 unit of **Chain-2**, XPS, EPR, and magnetic susceptibility measurements were carried out. Figure 2 shows XPS spectra of the Pt 4f and Rh 3d regions for **2** and **Chain-2** at room temperature, whose binding energies (eV) are

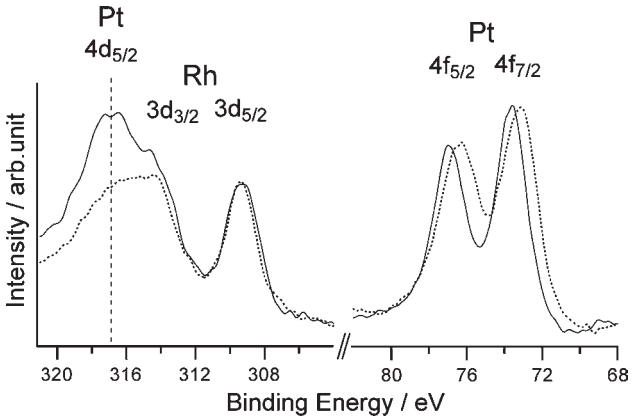

Figure 2. Rh $3d_{3/2}$ and $3d_{5/2}$ (left) and Pt $4f_{5/2}$ and $4f_{7/2}$ (right) core levels of XPS for **2** (dotted lines) and **Chain-2** (solid lines) at room temperature.

Table 3. Binding Energies (eV) for the 3d Region of Rhodium and the 4f Region of Platinum in **2** and **Chain-2**

	Rh $3d_{5/2}$	Pt $4f_{5/2}$	Pt $4f_{7/2}$
2	309.4	76.3	73.1
Chain-2	309.3	77.0	73.6

summarized in Table 3.[26] In the $3d_{3/2}$ region of Rh, Pt $4d_{5/2}$ signals also exist but are overlapped with the Rh signals. The Rh $3d_{5/2}$ core level spectra for rhodium(1+) compounds have been reported in the range of 307.6−309.6 eV, while rhodium(3+) compounds have been reported at 308.8−311.3 eV,[2j,27] and the observed peaks [309.4 (**2**) and 309.3 (**Chain-2**) eV] occur in both regions. The Pt $4f_{7/2}$ binding energy for **2** was determined as 73.1 eV, which is closer to that of the platinum(2+) complex $[Pt^{II}_2(en)_2(\alpha\text{-pyridonato})_2](NO_3)_2$ (72.6 eV; en = ethylenediamine) than to that of the platinum(3+) complex $[Pt^{III}_2(NH_3)_4(\alpha\text{-pyrrolidonato})_2(NO_3)_2](NO_3)_2$ (75.0 eV),[9b] suggesting that the oxidation state of the Pt−Rh dinuclear complex **2** is Pt^{2+}−Rh^{3+}.[13b] Although the Pt $4f_{7/2}$ binding energy for **Chain-2** (73.6 eV) is also closer to that of Pt^{2+}, both Pt $4f_{7/2}$ and $4f_{5/2}$ for **Chain-2** are more shifted than those of **2** (Figure 2, right), which might be caused by a higher degree of spectral overlap of the Pt^{2+} and Pt^{3+} peaks.[3a−c,9b] Hence, it can be concluded that **Chain-2** exhibits a mixed valency of Pt^{2+} and Pt^{3+}.

As will be described in detail in the EPR Spectra section, the EPR spectrum of **Chain-2** with a relatively small g_{av} value (g_{av} = 2.01 at room temperature) was

(23) (a) Mehran, F.; Scott, B. A. *Phys. Rev. Lett.* **1973**, *31*, 99–102. (b) Mehran, F.; Scott, B. A. *Phys. Rev. Lett.* **1973**, *31*, 1347–1349.

(24) Bunn, A. G.; Wayland, B. B. *J. Am. Chem. Soc.* **1992**, *114*, 6917–6919.

(25) (a) Barton, J. K.; Caravana, C.; Lippard, S. J. *J. Am. Chem. Soc.* **1979**, *101*, 7269–7277. (b) Arrizabalaga, P.; Castan, P.; Geoffroy, M.; Laurent, J.-P. *Inorg. Chem.* **1985**, *24*, 3656–3660.

(26) The results of **2** were reported in ref 13b.

(27) Frederick, B. G.; Apai, G.; Rhodin, T. N. *J. Am. Chem. Soc.* **1987**, *109*, 4797–4803.

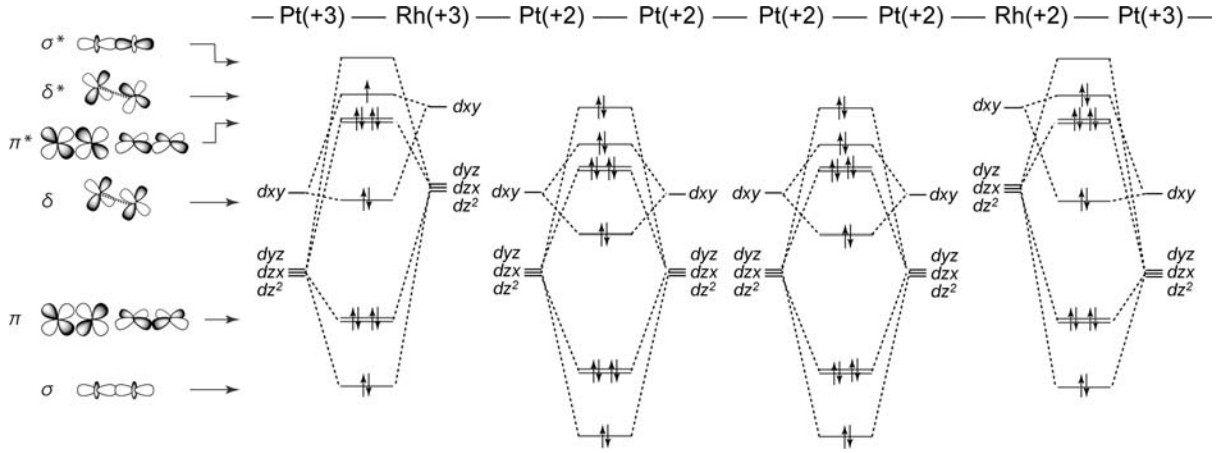

Figure 3. Schematic molecular orbital diagram of **Chain-2**. The figure is not based on the calculation results, and the interactions between each dinuclear unit are not considered in the figure.

obtained, indicating the existence of an unpaired electron. The magnetic susceptibility of **Chain-2** has a μ_{eff} [$\propto(\chi T)^{1/2}$] value of 1.86 at 265 K, showing one unpaired electron per Pt_6Rh_2 unit (Figure S4 in the Supporting Information). As mentioned previously, the results of single-crystal X-ray and elemental analysis for **Chain-2** indicate that the total metal charge for the Pt_6Rh_2 unit is 19+. Furthermore, the results of XPS, EPR, and magnetic susceptibility measurements show that **Chain-2** contains one unpaired electron per Pt_6Rh_2, where the Pt atoms exhibit a mixed valency of Pt^{2+} and Pt^{3+}. Figure 3 shows a schematic view of the molecular orbital diagram of **Chain-2**. Only considering d-orbital overlaps between corresponding pairs, three types of bonding and antibonding combinations in the order $\sigma < \pi < \delta < \delta^* < \pi^* < \sigma^*$ can be obtained.[28] In both dinuclear complexes [Pt−Rh] and [Pt−Pt], the d_{xy} orbital is higher in energy than d_{z^2} because π interactions with the amidate ligands induce a reversal of δ^* and π^*, resulting in the order $\sigma < \pi < \delta < \pi^* < \delta^* < \sigma^*$.[29] In addition, it is expected that each combination in [Pt−Rh] is higher than that in [Pt−Pt]. Taking into account the total metal charge (19+) and mixed valency of Pt atoms, the reasonable diagram shown in Figure 3 was obtained. HOMO (SOMO) resides in δ^* of the [Pt−Rh] complexes. The SOMO in **Chain-2** is attributed to δ^*, satisfying the small g_{av} value obtained by EPR,[30] similarly to that for **Chain-1**.[10]

The results of calculations also support this electronic structure. Figure 4 shows the first and second HOMOs in the model compound $[\{PtRh(PVM)_2(NH_3)_2Cl_2\}_2\{Pt_2(PVM)_2(NH_3)_4\}_2]^{6+}$, which is obtained from the crystal

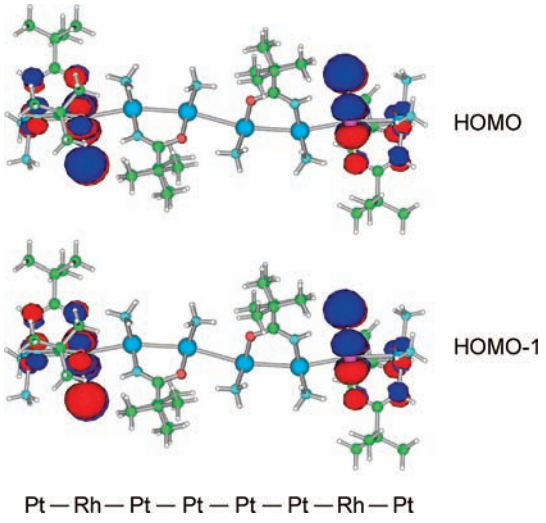

Figure 4. Shape of the first and second HOMOs in **Chain-1** without axially coordinated Cl^- ions.

structure of **Chain-1** without axially coordinated Cl^- ions. Both molecular orbitals occupy large regions around both sides of the [Pt−Rh] complexes, and both HOMO levels are degenerate with an energy of −17.46 eV.[31] Although it is impossible to perform an accurate calculation on the model compound $[\{PtRh(TCM)_2(NH_3)_2Cl_2\}_2\{Pt_2(PVM)_2(NH_3)_4\}_2]^{6+}$ for **Chain-2** because of the lower crystallographic symmetry, the estimated HOMO in $[\{PtRh(PVM)_2(NH_3)_2Cl_2\}_2\{Pt_2(PVM)_2(NH_3)_4\}_2]^{6+}$ is substantially consistent with that in the molecular orbital diagram (Figure 3). Taking into account all of the results, the oxidation states of the octameric unit in both **Chain-1** and **Chain-2** are approximately expressed as $Pt^{3+}-Rh^{2.5+}-Pt^{2+}-Pt^{2+}-Pt^{2+}-Pt^{2+}-Rh^{2.5+}-Pt^{3+}$. The unpaired electron occupying the Rh d_{xy} orbitals (δ^* orbitals in the Pt−Rh dinuclear parts) hops from one Rh atom to another in the Pt_6Rh_2 unit.[10] To our knowledge, these characteristic chains, **Chain-1** and **Chain-2**, are the first examples of 1D metal complexes that do not have σ^* orbitals as the HOMO, instead having δ^* orbitals.[1−3]

EPR Spectra. The spin hopping in **Chain-2** is very characteristic, considering the relatively large separations of the adjacent Rh ions (13.78 Å within the octameric unit

(28) Cotton, F. A.; Murillo, C. A.; Walton, R. A. *Multiple Bonds between Metal Atoms*, 3rd ed.; Springer Science and Business Media, Inc.: New York, 2005.

(29) Kawamura, T.; Katayama, H.; Nishikawa, H.; Yamabe, T. *J. Am. Chem. Soc.* **1989**, *111*, 8156–8160.

(30) If the g_{av} value obtained for **Chain-2** is interpreted in terms of a d_{z^2} hole state (the case for both Pt^{3+} and Rh^{2+}) with an admixture of the lower-lying d_{xz} and d_{yz} states because of spin−orbit coupling, a larger g_{av} value is expected.

(31) The third HOMO in **Chain-1** occupies a σ/σ^* orbital over the octameric unit with an energy of −17.75 eV. DFT calculations were also performed on the model $[\{PtRh(PVM)_2(NH_3)_2Cl_3\}_2\{Pt_2(PVM)_2(NH_3)_4\}_2]^{4+}$ with axially coordinated Cl^- ions. In that case, because of axial coordination, the σ/σ^* orbital is raised to be the HOMO (−12.96 eV), while the degenerate δ^* orbitals around both sides of the [Pt−Rh] complexes are the second and third HOMOs with an energy of −13.11 eV.

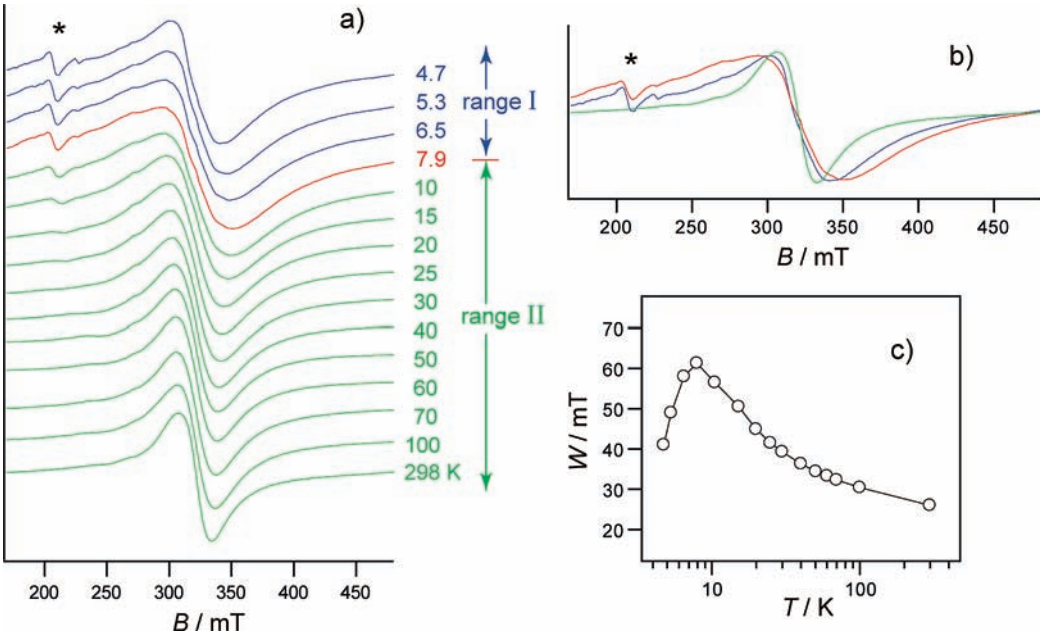

Figure 5. (a) Continuous-wave EPR spectra of powder samples of **Chain-2** in the temperature range 4.7−298 K. (b) Selected spectra of **Chain-2** at 4.7 (blue), 7.9 (red), and 298 (green) K. Asterisks correspond to unidentified impurities. (c) Plots of the peak-to-peak line width (W, mT) vs temperature (K).

Table 4. Temperature Dependences of g Values and Peak-to-Peak Line Widths (W, mT) Observed in EPR Spectra of **Chain-2**[a]

temperature (K)	g value	peak-to-peak line width (W, mT)
4.7	2.01	41.0
5.3	2.01	49.0
6.5	2.03	58.0
7.9	2.03	61.3
10	2.02	56.5
15	2.01	50.5
20	2.01	44.9
25	2.01	41.5
30	2.01	39.3
40	2.00	36.3
50	2.00	34.4
60	2.00	33.3
70	2.01	32.3
100	2.01	30.4
298	2.01	26.0

[a] Experimental settings: microwave frequency, 9.0223 (4.7 K), 9.0224 (5.3 K), 9.0204 (6.5 K), 9.0187 (7.9 K), 9.0168 (10 K), 9.0159 (15 K), 9.0157 (20 K), 9.0156 (25 K), 9.0155 (30 K), 9.0154 (40 K), 9.0153 (50 K), 9.0152 (60 K), 9.0152 (70 K), 9.0154 (100 K), and 9.4346 (298 K) GHz; microwave power, 5 mW; field modulation (100 kHz), 1 mT.

and 10.33 Å between the neighboring units in **Chain-2**) and the nature of the spin orbital perpendicular to the metal−metal bond axis. The variable-temperature EPR measurements (T = 4.7−298 K) for the powder sample of **Chain-2** showed a broad isotropic signal without a hyperfine structure over the whole temperature range (Figure 5). In most EPR spectra of amidate-bridged dinuclear mixed-valent rhodium(II,III) complexes or various other mixed-valent complexes of any transition metals,[32] anisotropic EPR signals based on the metal d orbital are observed, and only in a very few exceptional cases are isotropic signals reported, which are, however, the result of hopping on the ligand radicals.[32b,c] The g values of **Chain-2** are always close to 2.0 (Table 4), and the peak-to-peak line width (W, mT) increases with an increase of the temperature in range I (T = 4.7−7.9 K), whereas W decreases with an increase of the temperature in range II (T = 7.9−298 K). Such temperature dependence is attributed to spin hopping and coalescence (range I) and motional narrowing (range II) in EPR spectroscopy.[3h,33] The electron-hopping frequency monotonically increases with an increase of the temperature over the whole temperature range. However, because of exchange and coalescence, the signal broadens with an increase of the temperature in range I, and eventually the line width reaches a maximum at 7.9 K. As shown in Figure 5, a broader spectrum at 7.9 K does not exhibit the separated profile due to the two sites but overlapped one with a slightly different g value, whereas at temperatures above 7.9 K (range II), the signal becomes narrower with an increase of the temperature because of motional narrowing.[3h,33]

The hopping frequency (ω) is comparable to the characteristic frequency (ω_c) at 7.9 K and increases further above 7.9 K. Assuming that the coalescence and narrowing are due to hopping between sites that differ in the orientation of the g tensor and that the g difference (Δg) between the sites is typically ∼0.1,[34] we can estimate the

(32) (a) Kawamura, T.; Fukamachi, K.; Sowa, T.; Hayashida, S.; Yonezawa, T. *J. Am. Chem. Soc.* **1981**, *103*, 364–369. (b) Kasack, V.; Kaim, W.; Binder, J. H.; Jordanov, J.; Roth, E. *Inorg. Chem.* **1995**, *34*, 1924–1933. (c) Kawamura, T.; Kachi, H.; Fujii, H.; Kachi-Terajima, C.; Kawamura, Y.; Kanematsu, N.; Ebihara, M.; Sugimoto, K.; Kuroda-Sowa, T.; Munakata, M. *Bull. Chem. Soc. Jpn.* **2000**, *73*, 657–668.

(33) (a) Anderson, P. W.; Weiss, P. R. *Rev. Mod. Phys.* **1953**, *25*, 269–276. (b) Slichter, C. P. *Principles of Magnetic Resonance, Springer Series in Solid-State Sciences*; Flude, P., Ed.; Springer-Verlag: New York, 1978. (c) Bencini, A.; Gatteschi, D. *Electron Paramagnetic Resonance of Exchange Coupled Systems*; Springer-Verlag: Berlin, 1990. (d) Seth, J.; Palaniappan, V.; Johnson, T. E.; Prathapan, S.; Lindsey, J. S.; Bocian, D. F. *J. Am. Chem. Soc.* **1994**, *116*, 10578–10592. (e) Tanaka, H.; Kuroda, S.-i.; Yamashita, T.; Mitsumi, M.; Toriumi, K. *J. Phys. Soc. Jpn.* **2003**, *72*, 2169–2172.

(34) The typical value of 0.1 for the g difference between sites is proper in our case, considering that the ∼20 mT peak shift would be expected when the g value changes by ±0.1. At 7.9 K, the spectrum with a slightly different g value does not exhibit the separated profile due to the two sites but an overlapped one.

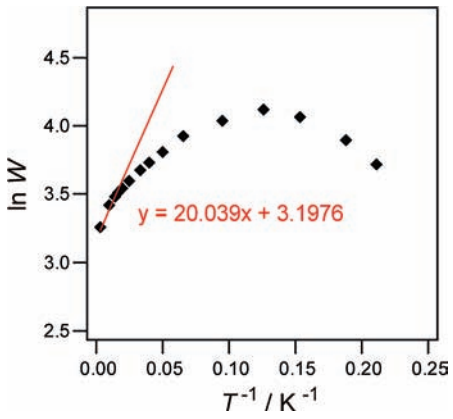

Figure 6. Plots of the logarithm of the peak-to-peak line width (W, mT) vs T^{-1} (K^{-1}). The red line exhibits $\ln \Delta\omega = E/kT + \ln(\omega_p{}^2\tau_\infty/2\pi)$ based on the relations $\Delta\omega \approx \omega_p{}^2/\omega$ (valid for $\omega_c \ll \omega$ and $T = 70-298$ K) and $\omega = 2\pi/\tau = (2\pi/\tau_\infty)\exp(-E/kT)$, where $\Delta\omega$ is the line width, ω_p is the static line width, τ is the hopping time constant, τ_∞ is τ at sufficiently high temperature, and E is the activation energy.

order of ω_c as 10^9 Hz, based on the equation $\omega_c \approx (\Delta g/g) \times 2\pi f(\mathrm{EPR})$,[33b] where f(EPR) is the EPR frequency. From the relations $\Delta\omega \approx \omega_p{}^2/\omega$[33a] (valid for $\omega_c \ll \omega$) and $\omega = 2\pi/\tau = (2\pi/\tau_\infty)\exp(-E/kT)$,[33c] where $\Delta\omega$ is the line width, ω_p is the static line width, τ is the hopping time constant, and τ_∞ is τ at sufficiently high temperature, the activation energy E is calculated as $\sim 2 \times 10$ K (~ 14 cm^{-1}; Figure 6); another simpler relation based on the equation $k_c = (kT_c/h)\exp(-E/RT_c)$, i.e., $E = 19.14T_c[10.32 + \log(T_c/k_c)]$ J mol^{-1},[33c] where T_c and k_c are the coalescence temperature and hopping rate, respectively, gives a calculated activation energy of $\sim 3 \times 10$ K (~ 21 cm^{-1}).

Temperature-dependent spectral line broadening and coalescence phenomena are often observed in NMR spectroscopy[33b,c] and sometimes observed in other spectroscopies.[35] These phenomena depend on the relationships of the time domains between molecular/electron dynamics and instruments (NMR, $10^{-1}-10^{-6}$ s; EPR, $10^{-4}-10^{-9}$ s; IR, picoseconds).[35,36] To date, electron fluctuations in mixed-valent metal complexes have been observed by visible (near-IR) spectroscopy to determine the electron-transfer dynamics.[37] Moreover, intervalence charge transfers have also been observed as a coalescence of ligand vibrational peaks in IR spectroscopy;[35] however, those spectroscopic techniques are difficult to apply to slower electron dynamics, as observed in our case.

Conclusion

This work was devoted to the synthesis and characterization of a novel mixed-valent 1D complex, **Chain-2**. We succeeded in obtaining **Chain-2** by simply mixing the dinuclear [Pt−Pt] complex **1** and the [Pt−Rh] complex **2**, resulting in substitution of the ligands from PVM (**Chain-1**) to TCM (**Chain-2**). The result implies the possibility of modifying this type of unique heterometallic 1D complex, −[Pt−Rh]−[Pt−Pt]−[Pt−Pt]−[Rh−Pt]−Cl−, with other organic ligands. The results of XPS, EPR, and magnetic susceptibility measurements and DFT calculations showed that the oxidation state of the octameric unit in **Chain-2** is $Pt^{3+}-Rh^{2.5+}-Pt^{2+}-Pt^{2+}-Pt^{2+}-Pt^{2+}-Rh^{2.5+}-Pt^{3+}$, where the HOMO (SOMO) consists of δ^* of Pt−Rh dinuclear parts with an unpaired electron hopping between the Rh atoms. By changing the bridging ligand from PVM (**Chain-1**) to the less electron-donating TCM (**Chain-2**), although a clear effect on the electronic structure was not observed, stable crystals for several measurements were obtained.

Acknowledgment. This work was supported by the Grants-in-Aid for Scientific Research (Young Scientist (B) Grant 19750048), Mitsubishi Chemical Corporation Fund, Kinki Invention Center, and Yazaki Memorial Foundation for Science & Technology. Theoretical calculations were performed using the Research Center for Computational Science, Okazaki, Japan.

Supporting Information Available: X-ray crystallographic files (CIF) for **Chain-2**, ESI-MS spectrum for **Chain-2** in MeOH, IR and UV−vis spectra, and magnetic susceptibility for **Chain-2**. This material is available free of charge via the Internet at http://pubs.acs.org.

(35) (a) Grevels, F.-W.; Jacke, J.; Klotzbucher, W. E.; Kruger, C.; Seevogel, K.; Tsay, Y.-H. *Angew. Chem., Int. Ed.* **1987**, *26*, 885–887. (b) Wu, R.; Koske, S. K. A.; White, R. P.; Anson, C. E.; Jayasooriya, U. A.; Cannon, R. D. *J. Chem. Soc., Chem. Commun.* **1994**, 1657–1658. (c) Ito, T.; Hamaguchi, T.; Nagino, H.; Yamaguchi, T.; Washington, J.; Kubiak, C. P. *Science* **1997**, *277*, 660–663. (d) Ito, T.; Hamaguchi, T.; Nagino, H.; Yamaguchi, T.; Kido, H.; Zavarine, I. S.; Richmond, T.; Washington, J.; Kubiak, C. P. *J. Am. Chem. Soc.* **1999**, *121*, 4625–4632. (e) Londergan, C. H.; Kubiak, C. P. *Chem.—Eur. J.* **2003**, *9*, 5962–5969. (f) Crutchley, R. J. *Angew. Chem., Int. Ed.* **2005**, *44*, 6452–6454. (g) Salsman, J. C.; Kubiak, C. P.; Ito, T. *J. Am. Chem. Soc.* **2005**, *127*, 2382–2383. (h) Ito, T.; Imai, N.; Yamaguchi, T.; Hamaguchi, T.; Londergan, C. H.; Kubiak, C. P. *Angew. Chem., Int. Ed.* **2004**, *43*, 1376–1381. (i) Lear, B. J.; Glover, S. D.; Salsman, J. C.; Londergan, C. H.; Kubiak, C. P. *J. Am. Chem. Soc.* **2007**, *129*, 12772–12779.

(36) Endicott, J. F. *Encyclopedia of Inorganic Chemistry*; John Wiley & Sons: New York, 1994; Vol. *3*, p 1084.

(37) Hush, N. S. *Prog. Inorg. Chem.* **1967**, *8*, 391–444.